Nanoscale

Accepted Manuscript

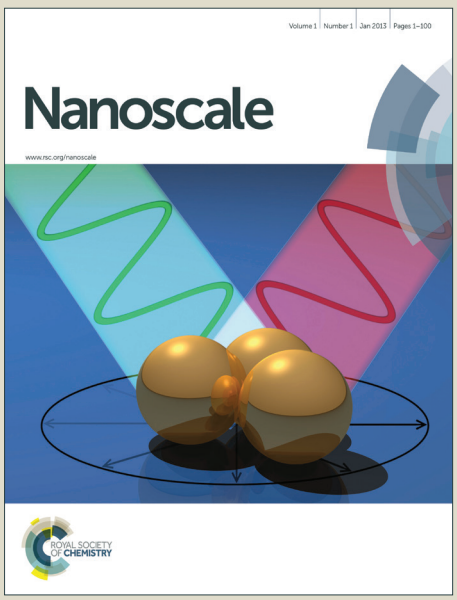

ROYAL SOCIETY OF CHEMISTRY

www.rsc.org/nanoscale

Journal Name

RSCPublishing

ARTICLE

Peptide Modified Gold Nanoparticles for Improved Cellular Uptake, Nuclear Transport, and Intracellular Retention

Cite this: DOI: 10.1039/xoxxoooooox

Received ooth January 2012,
Accepted ooth January 2012

DOI: 10.1039/xoxxoooooox

www.rsc.org/

C. Yang,[a] J. Uertz,[b] D. Yohan,[a] and B. D. Chithrani[a]*

Gold nanoparticles (GNPs) are being extensively used in cancer therapeutic applications due to their ability to act as both an anticancer drug carrier in chemotherapy and as a dose enhancer in radiotherapy. The therapeutic response can be further enhanced if nanoparticles (NPs) can be effectively targeted into the nucleus. Here, we present an uptake and removal of GNPs functionalized with three peptides. The first peptide (RGD peptide) enhanced the uptake, the second peptide (NLS peptide) enhanced the nuclear delivery, while the third one (pentapeptide) covered the rest of the surface and protected it from the binding of serum proteins onto the NP surface. The pentapeptide also stabilized the conjugated GNP complex. The peptide-capped GNPs showed a five-fold increase in NP uptake followed by effective nuclear localization. The fraction of NPs exocytosed was less for peptide-capped NPs as compared to citrate-capped ones. Enhanced uptake and prolonged intracellular retention of peptide-capped GNPs could allow NPs to perform their desired applications more efficiently in cells. These studies will provide guidelines for developing NPs for therapeutic applications, which will require "controlling" the NP accumulation rate while maintaining low toxicity.

Introduction

Nanotechnology-based approaches facilitate the further development of safer yet more effective diagnostic and therapeutic modalities for cancer therapy.[1-4] The primary goal of nanoparticle (NP)-based platforms will be the optimized delivery of therapeutics to tumours while causing minimum damage to normal tissue and side effects to the patient.[5-9] Among other NPs, Gold NPs (GNPs) are being used in cancer research due to their biocompatibility and ability to act as a radiosensitizer and as a drug carrier in cancer therapy.[10-14] The design of smart multifunctional nanocarriers in order to improve current therapeutic applications requires a thorough understanding of the mechanisms behind nanoparticles (NPs) entering and leaving the cells. For drug delivery and radiation therapy applications, it is necessary to control and manipulate the accumulation of NPs for an extended period of time within the cell. Previous studies have shown that both uptake and removal mechanisms are dependent on the size, shape, and surface properties of NPs. Among NP sizes between 13-100 nm, NPs of diameter 50 nm showed the highest cell uptake.[10, 15-17] Elucidating the mechanism of uptake and removal of NPs in cells could lead to a better understanding of NP toxicity. For example, if the NPs are trapped in vesicles and leave the cells intact, they are unlikely to induce cellular toxicity). Many theoretical calculations support the size dependent NP uptake.[18-20] A recent theoretical study has shown that the cellular uptake of NPs is also dependent on their elasticity in addition to their size.[21] Chithrani *et al.* have put forward a theoretical calculation to support the NP removal process.[16] In most of these studies, NPs took the endo-lyso path where NPs enter the cell through endocytosis, are trapped in endosomes, fuse with lysosomes for processing, and leave the cell *via* the exocytosis process. During the endo-lyso path, NPs were localized in either endosomes or lysosomes. Cell cytoplasm and nucleus were free of NPs. Recent studies have shown enhanced therapeutic effects when NPs were targeted into the nucleus[22]. Several approaches have been used for successful nuclear targeting of NPs as discussed in the next section.[23-26]

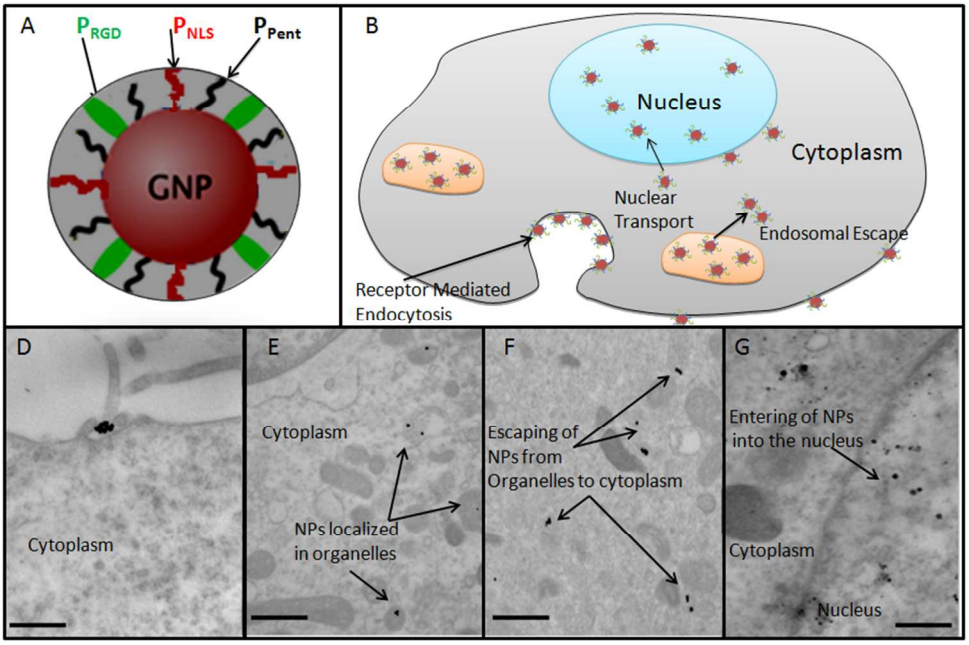

Fig. 1 Trajectory of peptide-conjugated GNPs through the cell. A, Schematic of a functionalized GNP used in the study. **B**, Trajectory of peptide-conjugated GNPs through the cell. **D-G**, Path of the NPs was captured using TEM images and is as follows: **D**, GNP-Peptide complex bound to the plasma membrane for entry into the cell *via* the endocytosis process, **E**, Internalized NPs were localized in vesicles, such as, endosomes and lysosomes, **F**, Escaping of NPs from vesicles into the cytoplasm, **G,** Entering the nucleus through NPC (scale bars = 100nm).

For successful targeted nuclear delivery, the NPs must escape endosomal pathways, and interact with the Nuclear Pore Complex (NPC) for entry into the nucleus as illustrated in Fig. 1. Furthermore, the NPs should be small enough to cross the nuclear membrane (<30 nm for import through nuclear pores).[27] In the past, scientists have used viruses to deliver genes to cell nuclei. There have been limited studies using NP-based non-viral vectors for targeting into the nucleus *via* peptide sequences derived from viruses.[23, 25, 28, 29] However, many of the peptides used on these non-viral vectors were more efficient on either cell entry or nuclear entry. Previous studies have shown that the combination of natural peptide sequences derived from viruses would be more competent as opposed to using a single peptide.[22, 23, 30] Multiple peptides were first assembled on a Bovine Serum Albumin (BSA) molecule followed by conjugation of BSA onto NP surface. This is a multi-step process which requires the purification of NPs through gel columns to remove reactants such as 3-maleimidobenzoic acid *N*-hydroxysuccinimide ester (MBS) and Dithiothreitol (DTT). In this study, we have shown how to assemble multiple peptides on the surface of GNPs using a two-step process. The cellular uptake and removal of peptide-conjugated NPs were also discussed using both quantitative and qualitative methods.

In this study, a combination of a natural peptide (derived from a virus) and two synthetic peptides on the same NPs were used. The synthetic peptide (P_{RGD}) contains a segment of basic lysine residues in addition to the integrin-binding domain (RGD) (peptide sequence: H-Cys-Lys-Lys-Lys-Lys-Lys-Lys-Gly-Gly-Arg-Gly-Asp-Met-Phe-Gly-OH). The lysine residues were added to mimic NLS peptides while the integrin-binding domain was employed to enhance cell entry. The integrins are a family of the transmembrane glycoproteins used by a number of viruses for the purpose of cell internalization.[31] This type of peptide is also referred to as a RME (receptor mediated endocytosis) peptide due to the enhanced cell delivery of NPs *via* the RME process.[23] However, it is also possible to avoid the RME process by using cell penetrating peptides (CPPs).[26] Brust and co-workers suggested the approach of evading the well-established endosomal pathway of uptake to a significant extent, either *via* the delivery of the NPs by liposomes or by surface modification of the NPs with the supposed cell penetrating peptides (CPPs).[26] However, the role of CPPs is not fully understood yet.The second peptide used in our study is a natural peptide (P_{NLS}), and has a nuclear localization signal (NLS) to facilitate nuclear entry. The sequence (H-Cys-Gly-Gly-Arg-Lys-Lys-Arg-Arg-Gln-Arg-Arg-Arg-Ala-Pro-OH) of P_{NLS} peptide originated from an adenovirus. The third peptide known as "pentapeptide (P_{Pent})" (Sequence: H-Cys-Ala-Leu-Asn-Asn-OH) was used to stabilize NPs for conjugation of the previously discussed peptides. Furthermore, it was used to protect NPs against serum proteins in tissue culture media. For example, our DLS and UV data showed that the size of the peptide-modified GNPs remains unaffected in the tissue culture media while the size of the citrate-capped GNPs changed due to the attachment of serum proteins (see the supplementary Figure S1). **Figure 1** illustrates the intracellular uptake and transport of peptide conjugated GNPs. Once NPs reach the cell membrane, they are wrapped up by the cell membrane (**Fig. 1C**), and internalized *via* the endocytosis process. Once internalized, NPs localize in organelles, such as endosomes and lysosomes (**Fig. 1D**). In order for these NPs to enter the nucleus, they must first escape from these organelles into the cytoplasm (**Fig. 1E**). Following this, the NPs bind to nuclear transport molecules, such as importin, *via* NLS peptides and enter through the nuclear pore complex (NPC) into the nucleus (**Fig. 1G**). This is the first time that a combination of RGD peptide, NLS peptide, and pentapeptide was used for nuclear targeting. The exocytosis of peptide-modified GNPs is not properly understood yet. Our study will focus on both uptake and removal of peptide modified GNPs.

Materials and methods

Synthesis of GNPs: GNPs of size 15 nm were synthesized using the citrate reduction method.[32, 33] First, 300 ml of 1% $HAuCl_4.3H_2O$ (Sigma-Aldrich) was added to 30 ml of double–distilled water and heated on a hot plate while stirring. Once it reached the boiling point, 600 µl of 1% anhydrous citric acid (Sigma-Aldrich) was added to form NPs 14 nm in diameter. After the color of the solution changed from dark blue to red, the solution was left to boil for another five minutes while stirring. Finally, the GNP solution was brought to room temperature while stirring.

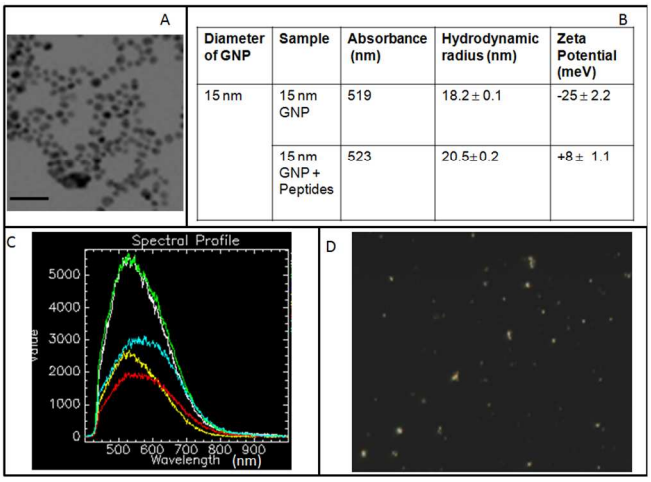

Diameter of GNP	Sample	Absorbance (nm)	Hydrodynamic radius (nm)	Zeta Potential (meV)
15 nm	15 nm GNP	519	18.2 ± 0.1	-25 ± 2.2
	15 nm GNP + Peptides	523	20.5±0.2	+8 ± 1.1

Fig. 2 Characterization of NPs. A, TEM image of citrate-capped GNPs. B, Table presenting the peak wavelength of UV-visible absorption, hydrodynamic radius, and zeta potential of citrate-capped and peptide-capped GNPs. C, Reflected spectra of GNPs. D, Darkfield image of GNPs. (scale bars = 100nm).

Peptide-GNP complex preparation: Peptide-GNP complexes were assembled by first conjugating the GNPs with H-Cys-Ala-Leu-Asn-Asn-OH (P_{Pent}) with approximately 300 peptides/GNP ratio for stabilization purposes. Following this,the peptide ($P_{RGD-NLS}$) with H-Cys-Lys-Lys-Lys-Lys-Lys-Lys-Gly-Gly-Arg-Gly-Asp-Met-Phe-Gly-OH sequence was added with an 8 to 10 peptide/GNP ratio. For nuclear targeted GNPs, P_{RGD} and P_{NLS} peptides (H-Cys-Gly-Gly-Arg-Lys-Lys-Arg-Arg-Gln-Arg-Arg-Arg-Ala-Pro-OH) were added in a 1:1 ratio since our initial optical studies have shown that the ratio of 1:1 of NLS and RGD peptide gave optimum cell internalization and nuclear localization.

Characterization of NPs: Nanoparticles were characterized using TEM, Dynamic Light Scattering (DLS), zeta potential measurements, and using optical reflectance as illustrated in **Fig. 2**. TEM images showed that the diameter of the NPs was approximately 15 nm. Zeta potential measurements displayed that naked or non-conjugated NPs were negatively charged while the peptide conjugated NPs were positively charged. GNPs have a strong reflectance spectrum (**Fig. 2C**) and were able to image (**Fig. 2D**) using this property. The stability of peptide-modified GNPs was verified using DLS and UV visible spectroscopy as illustrated in supplementary **Figure S1**.

Cell Culture and Particle Delivery: HeLa (cervical cancer cell line) cells were cultured in Dulbecco's Modified Eagle's Medium (DMEM) supplemented with 10% Fetal Bovine Serum (FBS). For optical imaging purposes, the cells were placed on glass coverslips, grown to 75%confluency, and then incubated with NP conjugates (10 nM) for six hours. Following the incubation, the coverslips were rinsed extensively with Phosphate-Buffered Saline (PBS). Subsequently, the cells were fixed with 4% paraformaldehyde in PBS for 15 min at room temperature and then rehydrated inPBS. Following fixation, the cover slip with cells were mounted onto glass slides and allowed to dry overnight prior to microscopy analysis.

Quantification of NP uptake and removal: To quantify NP uptake, following eight hours of incubation with GNPs, the cells were washed three times with PBS and trypsinized for quantification of GNPs present per cell. Cells were counted and then treated with HNO_3 at 200°C in an oil bath for ICP-AES analysis. To quantify NP removal, cells pre-incubated with NPs for eight hours were washed with PBS three times, introduced to fresh media supplemented with FBS, and left in the incubator for monitoring the exocytosis process. After one andsix hour time points, the cell were rinsed three times with PBS and trypsinized for quantification of GNPs present per cell. Cytotoxicity due to peptide-modified GNPs was compared to citrate-capped GNPs using the clonogenic assay (as illustrated in supplementary section **S2**). This assay can be used to measure the long term toxicity effects. In short term, we measured the cytotoxicity using trypan blue exclusion assay. There was no short-term or long-term cytotoxicity introduced by peptide modified NPs.

CytoViva Analysis of Cells with Internalized Nanoparticles: This CytoViva technology was specifically designed for optical observation and spectral confirmation of NPs as they interact with cells and tissues. Additional information regarding the CytoViva imaging technique is provided in the supplementary section **S3.** The illumination of the microscope system utilizes oblique angle lighting to create high signal-to-noise optimized darkfield based images. **Fig. 3A** is a darkfield image of a group of cells with internalized GNPs.

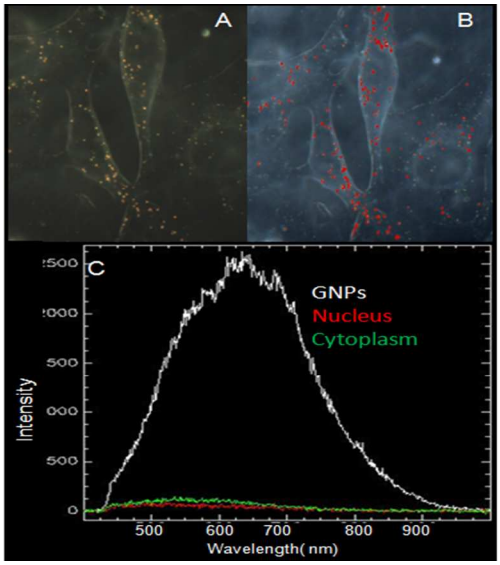

Fig. 3 CytoVivaHyperspectral imaging of GNPs internalized in cells. A, The darkfield image of GNPs in cells. B, The spectral angle map overlaid onto the hyperspectral darkfield image. The spectrum from each pixel is compared with reflectance spectra from gold, and if a match is determined, the pixels are coloured red. C, The reflectance spectra from one of the GNPs (white line) and the background reflectance from the nucleus (red line) and the cytoplasm (green line).

The GNPs appear bright owing to their high scattering cross-section. With the integrated CytoViva hyperspectral imaging capability, reflectance spectra from specific materials can be captured and

measured. The SAM (Spectral Angle Mapping) is an automated procedure used to determine whether GNPs are present in the input image, and locates which pixels contain the material of interest. SAM accomplishes these tasks by comparing unknown spectra in hyperspectral imagery with known spectra for the material of interest (GNPs in this case). The hyperspectral image displays the relative degree to which unknown spectra in each image pixel match the known GNP spectrum. **Figure 3B** shows the hyperspectral image with an overlaid spectral angle map where the red dots represent GNPs. **Figure 3C** illustrates the reflectance spectra from one of the red dots while the spectrum (white in colour) shows that it is quite similar to the reflectance spectrum of GNPs.[34, 35] The background reflectance spectra from the nucleus and cytoplasm are revealed. It can be clearly seen that the GNP clusters have a very high reflection compared to the background.

Results and Discussion

Characterization of GNP-peptide complexes: The size of the GNPs used in this study was approximately 15 nm in diameter. Larger NPs cannot travel through the nuclear pore complex (as discussed in the introduction section). The GNP–peptide complexes used in this study were prepared by assembling the three peptides (P_{NLS}, P_{RGD}, P_{Penta}) onto the NP surface. NP complexes were characterized using UV visible spectroscopy, DLS, and zeta potential measurements (see **Fig. 2**). There was no significant increase in terms of the size of NPs following conjugation with the peptide according to the DLS measurements (**Fig. 2B**). This was because the peptides are only few nanometres in size. However, the zeta potential changes from a negative value to a positive one (**Fig.2B**). The negative charge of the non-conjugated (citrate-capped) GNPs is due to the capping of the citrate molecules. Peptides are positively charged and GNPs were positively charged following conjugation with the peptides. The peptide-GNP complexes were tested for their stability in cell culture media before using them for cell uptake and transport studies. Nanoparticles were further characterised using their reflectance spectra as illustrated in **Fig. 2C,D**.

Cell uptake studies using peptide-GNP complex: Cellular uptake of peptide-GNP complexes was characterized using HeLa cells, a well-known human fibroblast epithelial cell line. The cellular uptake data proved that the cells targeted with a peptide containing RGD components had the highest NP uptake as compared to cells targeted with citrate-capped NPs (as made GNPs). It is believed that the synthetic peptide (P_{RGD}) with an integrin binding domain (RGD) supplemented an additional driving force for the cell entry of NPs. The increase in uptake of NPs functionalized with P_{Pent} alone could be due to their positive charge. Positively charged NPs have a higher uptake compared to negatively charged (citrated-capped) NPs.[36] Cell uptake was lower for NPs conjugated with both P_{NLS} and P_{RGD} as compared to NPs conjugated with P_{RGD} alone. This could be due to the reduction in the number of P_{RGD} present on the NP surface. The optimized ratio of peptides used was 1:1 for improving both NP

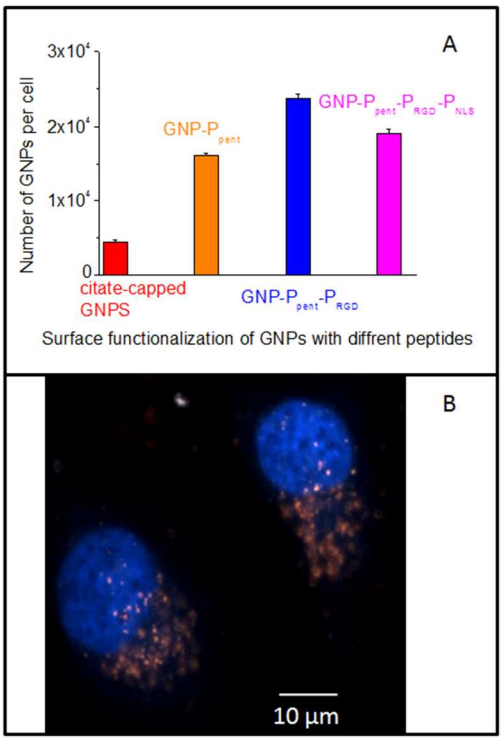

Fig. 4 NP uptake data for peptide conjugated GNPs. A, Cell uptake data corresponding to the presence of each peptide alone and the combined presence of three peptides on GNPs. B, CytoViva Hyperspectral imaging of cells internalized with GNPs functionalized with pentapeptide, NLS, and RGD peptides. The bright dots represent GNPs. The scale bar represents 10 µm.

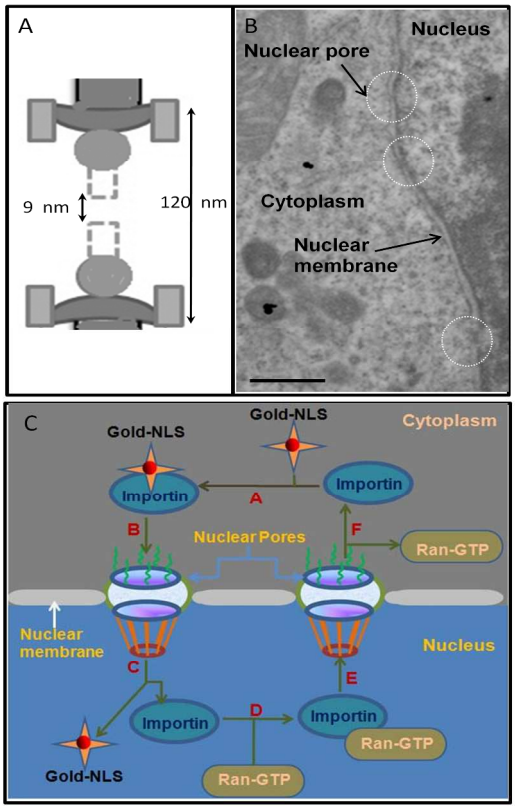

Fig. 5 Mechanism of nuclear transport GNP-peptide complex. A, Schematic illustrating the cross-section of the nuclear pore complex. B,TEM image showing few nuclear pores in the nuclear membrane. **C**, Mechanism of selective nuclear transport. GNP-peptide complexes, which possess a Nuclear Localization Signal (NLS), were bound to importin and were transported through the NPC. Mediators, such as the small GTPase Ran, play a vital role in both the GNP-peptide complex release and the recycling of importin into the cytoplasm through NPC.

internalization and nuclear localization. The combination of NLS and RGD enable effective cell entry and nuclear localization as illustrated in **Fig. 4**.

Mechanism of nuclear transport: One of the features that differentiate a eukaryotic cell from a prokaryotic cell is the presence of a nucleus. The nucleoplasm and the genetic material are separated from the cytoplasm by the nuclear envelope, a double membrane bilayer.[37, 38] The entry and exit of molecules from the nucleus is mainly through the Nuclear Pore Complex (NPC) (see **Fig. 5A, B**). Large proteinaceous assemblies, NPCs, are embedded throughout the nuclear membrane that forms selective channels perforating the double membrane surrounding the nucleus.[37] The role of these structures is to serve as sole mediators of nucleocytoplasmic exchange and transport of macromolecules with high specificity.[37, 39] NPC is a complex cylindrical structure with octagonal symmetry,

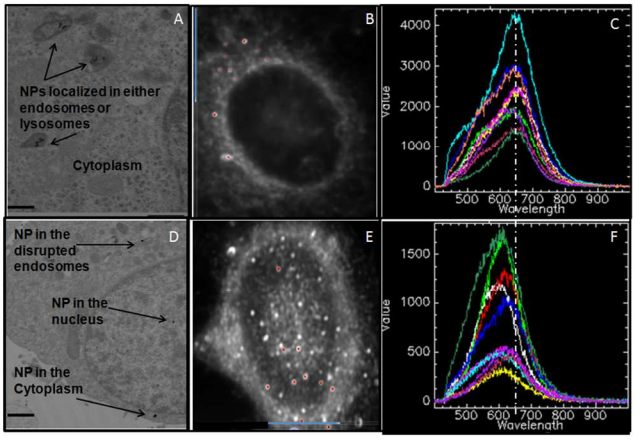

Fig. 6 TEM and Hyperspectral imaging of citrate-capped and peptide-GNPs internalized in cells. A, TEM image of citrate-capped (non-targeted) GNPs localized in either endosomes or lysosomes. B, Darkfield image of a cell internalized with non-targeted GNPs. C, Reflected spectra collected from few GNPs clusters (marked red in image B). D, TEM image of peptide-capped (nuclear-targeted) GNPs localized in either disrupted endosomes or cytoplasm. E, Darkfield image of a cell internalized with nuclear-targeted GNPs. F, Reflected spectra collected from few GNPs clusters (marked red in image E). (Scale bar = 100 nm).

100-150 nm in diameter, 50-70 nm in thickness, and 125 million Dalton in mass depending on the organism[38].The number of NPCs varies from around 3000-4000 per nucleus, depending on the activity level of a cell.[40] A core structure containing eight spokes surrounding a central tube is present within each NPC.[38] Peripheral filaments are attached to the core and form a basket-like structure on the nuclear side of the complex.[38] Passive diffusion of ions, water and small proteins of less than 60 kDa occur through longitudinal channels (10 nm diameter and 50 nm in length form)localized between spokes.[40] The transport of larger particles occur through energy dependent active transport *via* specific receptor proteins.[40] The pore gate is a dynamic structure and opens up to approximately 30 nm.[38, 40]

Transport of macromolecules across the NPC require specific amino acid sequence spans, known asNuclear Localization Sequences (NLSs).[38] Karyopherins, such as importins, are required to bring cargo to the NPCs[38].Karyopherins can bind the cargoes directly or *via* an adaptor protein.[38, 41, 42] The import substrate binds to the importin in the cytoplasm, which then docks to the cytoplasmic periphery of the NPC. The substrate-importin unit is subsequently translocated to the nuclear side of the NPC, mediated by the Ran GDP/GTP cycle.[41] The translocation is terminated on the nuclear side of the NPC which is followed by direct binding of Ran-GTP to importin that causes dissociation between the substrate and the importin.[41] The importin is exported back to the cytoplasm and the cycle continues (see **Fig. 5C**).[38, 41]

Although small molecules (less than 9 nm in diameter) can enter the nucleus without regulation, larger molecules (greater than 39 nm in diameter) such as NPs, require association with importin to enter the nucleus *via* an active transport process. Peptide-GNP complexes, which must be imported to the nucleus from the cytoplasm, should carry NLS for binding to importin as illustrated in **Fig. 5C**. The importin proteins in the cytoplasm bind to the NLS peptide on the peptide-GNP complexes, after which they are able to interact with the NPC to subsequently pass through its channel. Once NPCs are inside the nucleus, the interaction with Ran-GTP produces a conformational change in the importin, thus causing it to dissociate from its GNP complex. Importin proteins, which act as receptors for nuclear transport, recycle back into the cytoplasm resembling the recycling process of cell membrane receptors.

Distribution of citrate-capped and peptide-capped GNPs within cells: We have investigated the variation of NP distribution in cells internalized with citrate-capped and peptide-capped NPs using TEM and hyperspectral imaging. The citrate-capped GNPs travel through the regular endo-lyso path causing NPs to become trapped in either endosomes orlysosmes as clusters in the cytoplasm (**Fig. 6A**). TEM images confirmed that NPs were not localized in the nucleus. **Fig. 6B** is a darkfield hyperspectral image plane taken across a nucleus of a cell incubated with citrate-capped NPs. Nanoparticles were not localized in the nucleus as expected. **Fig. 6C** shows that the reflected spectra from few NP clusters peaked around 650 nm. The bottom panel of **Fig. 6**illustrates the cellular distribution of peptide-conjugated NPs. As illustrated in **Fig. 6D**, most of the NPs were

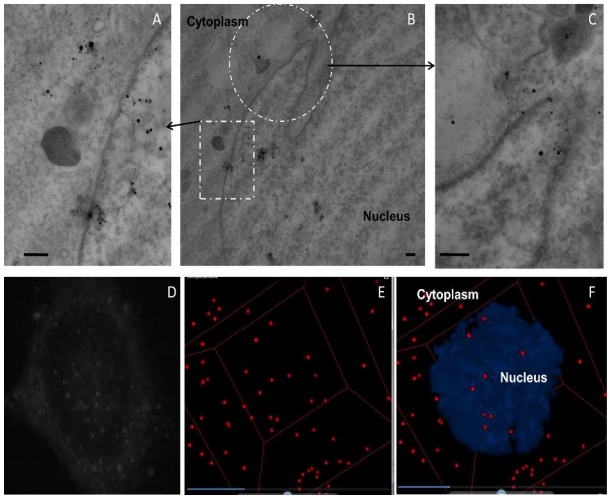

Fig. 7 2D and 3D view of localization of peptide-capped GNPs within the cell. A-C, Two dimensional (2D) view of localization of peptide-modified GNPs in the cytoplasm and nucleus using TEM imaging. A and C are insets of B. D-F, Hyperspectral imaging of a cell targeted with peptide-conjugated GNPs. D, Darkfield image of the cell used for three dimensional (3D) rendering. E, 3D view of the NPs localized in the cells. Red dots represent GNPs. F, Nucleus (blue in colour) is added to show the co-localization. (Scale bar = 100 nm).

either in disrupted endosomes, cytoplasm, or in the nucleus. **Figure 6E** is a darkfield hyperspectral image plane taken across a nucleus of a cell incubated with peptide-capped NPs. It clearly demonstrates the localization of NPs within the nucleus. **Fig. 6F** displays that the

reflected spectra from few NPs peaked around 600 nm. This blue shift of the spectra indicates that NPs are not clustered together. However, in the case of citrate-capped ones, NPs were clustered together in the endosomes or lysosomes, as illustrated in TEM images (**Fig. 6 A, D**). **Figure 7** further illustrates the NP distribution for peptide-conjugated GNPs. The top panel in **Fig.7** shows TEM images of GNPs localized in the cytoplasm and nucleus. The bottom panel displays the three dimensional (3D) distribution of NPs within a cell. **Figure 7D** is a darkfield image of a cell chosen for 3D mapping of the NP distribution. The white dots represent NPs localized in a particular image panel. A stack of imaging planes was acquired in the Z direction to cover the full height of the cells. All stacks were acquired with the CytoViva 3-D acquisition software. The stacks were deconvolved and the GNPs were identified using the CytoViva 3-D Analysis Software. Figure 7E displays the 3D distribution of GNPs within the cell shown in **Fig. 7D**. The red dots represent GNPs. The nucleus (marked in a blue colour) was introduced in the **Fig. 7F** to show that NPs were inside the nucleus as well. This is a novel imaging technique that can be used to image GNPs without using any optical probes. This is the first time that such a 3D distribution of nuclear targeted NPs was obtained.

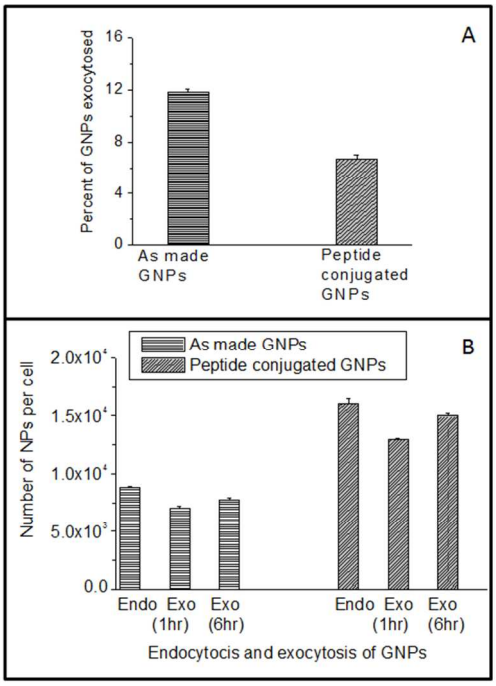

Fig. 8. **Exocytosis of peptide-capped GNPs**. A, Percent of NPs exocytosed for cells incubated with citrate-capped and peptide-capped GNPs. B, Dynamics of exocytosis process following one and six hours.

Exocytosis of peptide-conjugated GNPs: Previous work has shown that the exocytosis process depends on the cell type, NP size, and surface properties of NPs.[16, 43] Hence, the assessment of exocytosis has to be performed forevery specific condition. The exocytosis of GNPs functionalized with nuclear targeting peptides is not properly known yet. Our studies have shown for the first time that the fraction of NPs exocytosed was lower by two-fold for cells targeted with peptide-conjugated NPs (**Fig. 8A**). Additional experimental results on the exocytosis of particles coated with pentapeptide, NLS, and RGD peptides are illustrated in the supplementary Figure **S4**. Citrate-capped and pentapeptide NPs were localized in endosomes followed by processing *via* fusion with lysosomes.[16, 26] NPs localized in lysosomes are excreted into the extracellular matrix through fusing with the cell membrane. However, most of the GNPs capped with RGD and NLS peptides were able to enter the cytoplasm and reach the nucleus. Previous studies have shown that NPs localized in the cytoplasm or nucleus showed lower excretion from the cell.[44,45] Our results are in agreement with previously published work. For example, Wang *et al*. evaluated the excretion of CuO NPs in A549 cells and discovered that a portion of NPs, which were located in mitochondria and nucleus, could not be excretedby the cells.[44] Similarly, based on findings by Chu *et al*., clusters ofsilica NPs in lysosomes are more easily exocytosed by H1299 cells compared to single NPs in the cytoplasm.[45] We evaluated the exocytosis process as a function of time. As illustrated in Fig. 8B, a significant portion of the NPs were able to re-enter the cells. The percent of NPs re-entering the cells was 10% and 15% respectively, for citrate-capped (non-targeted) and peptide-capped (nuclear targeted) NPs. Nuclear targeted NPs seem to aggregate less within the cell (see **Fig. 6**). Hence, it is possible for these NPs to re-enter cells once excreted. This could be one of the reasons for an increase in NPs present in cells targeted with peptides following a prolonged exocytosis process. The enhanced retention of NPs within cells can be used for improved therapeutics in radiation therapy and chemotherapy as discussed in the introduction section. Our next goal is to use these NP complexes for combined cancer therapeutics since GNPs are being used as radiation dose enhancers and drug delivery vehicles.

Conclusions

Our results showed that the fuctionalization of GNPs with RGD peptide enhanced the NP uptake by five-fold. The combination of RGD peptide and NLS peptide allowed efficient nuclear targeting. Our studies showed that the fraction of NPs exocytosed was lower by a factor of two for cells targeted with peptide-conjugated NPs in comparison to citrate-capped (non-targeted) NPs. This prolonged intracellular retention of peptide functionalized NPs could allow NPs to exert their desired applications more efficiently in cells, especially in drug delivery. Hence, a proper understanding of endocytosis and exocytosis dynamics will shed more light on the design of GNPs in demand for cancer therapeutic applications.

Acknowledgements

The authors would like acknowledge Natural Sciences and Engineering Research Council of Canada (NSERC) and Ryerson University for their financial support.

Notes and references

[a] Department of Physics, Ryerson University, 350 Victoria Street, Toronto, ON, Canada, M5B 2K3,

[b] CytoVivaInc, 570 Devall Drive, Auburn, AL, USA, 36832.

1 M. E. Davis, Z. Chen and D. M. Shin, *Nat. Rev. Drug Discov.*, 2008, **7**, 771-782.
2 A. G. Cuenca, H. Jiang, S. N. Hochwald, M. Delano, W. G. Cance and S. R. Grobmyer, *Cancer*, 2006, **107**, 459–466.
3 J. Rao, *ACS Nano*, 2008, **2**, 1984–1986.
4 M. Ferrari, *Nat. Rev. Cancer* 2005, **5**, 161–171.
5 P. Alivisatos, *Nat. Biotech.*, 2003, **22**, 47-51.
6 M. Liong, J. Lu, M. Kovochich, T. Xia, S. G. Ruehm, A. E. Nel, F. Tamanoi and J. I. Zink, *ACS Nano*, 2008, **2**, 889-896.
7 S. Langereis, J. Keupp, J. L. J. van Velthoven, I. H. C. de Roos, D. Burdinski, J. A. Pikkemaat and H. Grüll, *J. Am. Chem. Soc.*, 2009, **9**, 1380-1381.
8 S. D. Perrault, C. Walkey, T. Jennings, H. C. Fischer and W. C. W. Chan, *Nano Lett.*, 2009, **9**, 1909-1985.
9 J. E. Lee, N. Lee, H. Kim, J. Kim, S. H. Choi, J. H. Kim, T. Kim, I. C. Song, S. P. Park, W. K. Moon and T. Hyeon, *J. Am. Chem. Soc.*, 2010, **132**, 552-557.
10 B. D. Chithrani, *Mol. Membr. Biol.*, 2010, **27**, 299-311.
11 B. D. Chithrani, *Insciences J.*, 2011, **1**, 136-156.
12 J. M. Bergen, H. A. van Recum, T. T. Goodman, A. P. Massey and S. H. Pun, *Macromol. Biosci.*, 2006, **6**, 506-516.
13 R. Shukla, V. Bansal, M. Chaudhary, A. Basu, R. R. Bhonde and M. Sastry, *Langmuir*, 2005, **21**, 10644-10654.
14 S. Jelveh and D. B. Chithrani, *Cancers*, 2011, **3**, 1081-1110.
15 B. D. Chithrani, A. A. Ghazani and W. C. W. Chan, *Nano Lett*, 2006, **6**, 662-668.
16 B. D. Chithrani and W. C. W. Chan, *Nano Lett.*, 2007, **7**, 1542-1550.
17 X. H. N. Xu, W. J. Brownlow, S. V. Kyriacou, Q. Wan and J. J. Viola, *Biochem.*, 2004, **43**, 10400-10413.
18 H. Gao, W. Shi and L. B. Freund, *Proc. Natl. Acad. Sci. U.S.A.*, 2005, **102**, 9469-9474.
19 W. Shi, Wang J, Fan Xan and Gao H, *Phy Rev E*, 2008, **78**, 061914.
20 S. Zhang, J. Li, G. Lykotrafitis, G. Bao and S. Suresh, *Adv. Mater.*, 2009, **21**, 419-424.
21 X. Yi, X. Shi and H. Gao, *Phy. Rev. Lett.*, 2011, **107**, 098101-098105.
22 C. Yang, M. Neshatian, M. Van Prooijen and B. D. Chithrani, *J. Nanosci. Nanotechnol.*, 2014, **14**, 4813–4819.
23 A. G. Tkachenko, H. Xie, D. Coleman, W. Glomm, J. Ryan, M. F. Anderson, S. Franzen and D. L. Feldheim, *J. Am. Chem. Soc.*, 2003, **125**, 4700–4701.
24 C. C. Berry, J. M. de la Fuente, M. Mullin, S. W. L. Chu and A. S. G. Curtis, *IEEE Trans. NanoBiosci.*, 2007, **6**, 262-269.
25 A. K. Oyelere, P. C. Chen, X. Huang, I. H. El-Sayed and M. A. El-Sayed, *Bioconjug. Chem.*, 2007, **18**, 1490-1497.
26 P. Nativo, I. A. Prior and M. Brust, *ACS Nano*, 2008, **2**, 1639-1644.
27 J. M. De la Fuente and C. C. Berry, *Bioconjug. Chem.*, 2005, **16**, 1176–1180.
28 A. G. Tkachenko, Y. Liu, D. Coleman, J. Ryan, W. R. Glomm, M. K. Shipton, S. Franzen and D. L. Feldheim., *Bioconjug. chem.*, 2004, **15**, 482-490.
29 B. Kang, M. K. Mackey and M. A. El-Sayed, *J Am Chem Soc*, 2010, **132**, 1517–1519.
30 J. A. Ryan, K. W. Overton, M. E. Speight, C. N. Oldenburg, L-N. Loo, W. Robarge, S. Franzen and D. L. Feldheim, *Anal. chem.*, 2009, **79**, 9150-9159.
31 G. Gregoriadis and B. McCormack, *Targeting of Drugs*, *Plenum Press, New York, London.*, 1st edn,1995.
32 G. Frens, *Nature*, 1973, **241**, 20-22.
33 G. T. Hermanson, *Bioconjugate Techniques*, Academic press, New York, U.S.A., 1996.
34 J. C. Y. Kah, K. W. Kho, C. G. L. Lee, C. J. R. Sheppard, Z. X. Shen, K. C. Soo and M. C. Olivo, *Int. J. Namomed.*, 2007, **2**, 785-798.
35 J. A. Viator, S. Gupta, B. S. Goldschmidt, K. Bhattacharyyal, R. Kannan, R. Shukla, P. S. Dale, E. Boote and K. Katti, *J. Biomed. Nanotechnol.*, 2010, **6**, 187-191.
36 E. Frohlich, *Int. J. Namomed.*, 2012, **7**, 5577-5591.
37 J. Fernandez-Martinez and M. P. Rout, *Curr. Opin. Cell Biol.*, 2009, **21**, 603-612.
38 S. R. Wente and M. P. Rout, *Cold Spring Harb. perspect. biol.*, 2010, **2**, a000562.
39 M. Suntharalingam and S. R. Wente, *Dev. cell*, 2003, **4**, 775-789.
40 M. Pavelka and J. Roth, *Functional Untrastructure*, Springer Vienna, 2010.
41 D. Görlich, *Curr. Opin. Cell Biol.*, 1997, **9**, 412-419.
42 L. F. Pemberton and B. M. Paschal, *Traffic*, 2005, **6**, 187-198.
43 D. Bartczak, T. Sanchez-Elsner, F. Louafi, T. M. Millar and A. G. Kanaras, *Small*, 2011, **7**, 388–394.
44 Z. Wang, N. Li, J. Zhao, J. C. White, P. Qu and B. Xing, *Chem. Res. Toxicol.,* 2012, **25**, 1512–1521.
45 Z. Chu, Y. Huang, Q. Tao and Q. Li, *Nanoscale*, 2011, **3**, 3291–3299.